

PREPARATION, CHARACTERIZATION AND SINTERING OF TI-35NB-7ZR-5TA ALLOY FOR BIOMEDICAL APPLICATIONS

Elisa Bueno Taddei

Instituto Tecnológico de Aeronáutica, ITA

São José dos Campos -SP, 12228-904

elisabtaddei@yahoo.com.br

Vinicius A. R. Henriques

AMR - Divisão de Materiais - Instituto de Aeronáutica e Espaço (IAE)

Centro Técnico Aeroespacial, São José dos Campos -SP, 12228-904

vinicius@iae.cta.br

Cosme R. M. da Silva

Instituto de Aeronáutica e Espaço (IAE)

Centro Técnico Aeroespacial, São José dos Campos -SP, 12228-904

cosme@iae.cta.br

Carlos Alberto A. Cairo

AMR - Divisão de Materiais - Instituto de Aeronáutica e Espaço (IAE)

Centro Técnico Aeroespacial, São José dos Campos -SP, 12228-904

ccairo@iae.cta.br

Abstract. *Titanium has become a widely used material for the manufacturing of osseointegrable implants because of its high corrosion resistance and excellent biocompatibility. Beta type titanium alloys have been developed in order to obtain low rigidity, which is considered effective for promotion bone healing and remodeling. The lowest elastic modulus that has been achieved to date is for the TNZT alloys based on the Ti-Nb-Zr-Ta system and a composition in this system is Ti-35Nb-7Zr-5Ta. Thus, Ti-35Nb-7Zr-5Ta alloy, which has low modulus of elasticity (55 GPa), was produced by powder metallurgy (PM), which is a favorable fabrication technique for titanium porous coating systems and present the advantage to provide good mechanical properties and stronger adhesion to the substrate. The Ti-35Nb-7Zr-5Ta samples were produced by the sintering of the elementary powders, in vacuum, between 800-1500 °C, with heating rate of 20 °C/min. All the powders were obtained by hydriding process and used in the hydrided form, aiming at the reduction of costs and increase of the sintering rate. In this work, results of the Ti-35Nb-7Zr-5Ta alloy production based in the microstructural evolution are presented. For the alloy microstructural characterization, scanning electron microscopy, Vickers microhardness measurements and bending strength, were used. Density was measured by Archimedes method. In this work an alternative blend method (with planetary mill) was used. The results show that a β -homogeneous microstructure is obtained in the whole sample extension with the increase of the sintering temperature.*

Keywords: Powder metallurgy, densification, microstructure, titanium

1. Introduction

The effort to find substitutions for repair of seriously damaged human bones dates back to centuries. Metals have been the primary materials in the past for this purpose due to their superior mechanical properties, albeit dangerous ions that are released in vivo from these alloys (Kalpana and Katti, 2004).

For implants the materials need to satisfy the all round properties of biocompatibility, strength and corrosion resistance, titanium is one of the best biocompatible metals and used most widely as implant. Titanium shows a minimal cellular reaction, in addition, when titanium is placed in contact with bones, it becomes firmly embedded in the bone. This situation is described as osseointegration (Wataria, *et al* (2004), Popa and Demetrescu, 2004).

However, for a metallic biomaterial, it is essential to have excellent mechanical properties too. The titanium high temperature β -phase has body-centered cubic (bcc) structure, while the α phase has a hexagonal close-packed (hcp) structure. β alloys as compared to $\alpha+\beta$ alloys, present an improved notched fatigue resistance and a superior resistance to wear and abrasion. These properties became β titanium alloys preferable to $\alpha+\beta$ alloys for biomedical applications and promising alloys for to a wide range of implant applications. Several β titanium alloys are already being used for biomedical

applications and further such alloys will be developed using the advantages of β titanium alloys (Eisenbarth *et al.* (2004)).

Ti-35Nb-7Zr-5Ta alloy due its high biocompatibility and lower modulus of elasticity is a promising candidate for implants fabrication, which has a β -like microstructure, an excellent combination of properties, including high resistance, excellent hot and cold workability and the lowest modulus of elasticity among the titanium alloys. The alloy processing by powder metallurgy eases the obtainment of parts with complex geometry (Long and Rack, 1998; Fujita *et al.* (1996)).

Powder metallurgy is in itself a complete materials processing route. Often the process begins with the reduction of ores to produce powder and the mixing of appropriate alloying additions. The homogeneity of composition is also assured down to the size of the powder particle itself. The powder agglomerates are then shaped into products with the application of pressure and temperature. When necessary, some additional processing steps such as forging are introduced as finishing operations (Cahn, Haasen and Kramer, 1991).

The technique has the unique advantage of successfully processing several alloys and compounds, which cannot be prepared by conventional melt techniques, especially in systems containing elements with remarkably different melting points. The material processed by P/M technique is free of coring and segregation which are commonly observed in parts produced by melting technique (Bora *et al.* (2004)).

P/M can broadly be divided into the following processing steps: production of powder; compaction and sintering, or hot pressing where compaction and sintering are combined into a single step. Sintering is the most common technique for consolidating powders. Essentially, it is the removal of the pores between the starting particles, combined with their growth and strong mutual bonding.

The powder metallurgy techniques can be carried out using blended elemental (BE) or prealloyed (PA) powders. The BE approach is potentially the lowest cost titanium P/M process available. Unfortunately, parts are limited in size and complexity, as well as less than 100% of theoretical density, which would adversely affect mechanical properties. Recent developments, such as using hydrided powders, have enabled the fabrication of BE parts to over 99% of full density, resulting in significantly improved properties. Porosity is an interesting feature in surgical implants system when good osteointegration conditions are necessary (Hurless and Froes, 2002).

2. Materials and Methods

The blended elemental method followed by a sequence of uniaxial and cold isostatic pressing with subsequent densification by sintering was chosen for the preparation of the alloy.

All the powders were obtained by hydriding method and sintered in hydrided state. For the titanium hydrided powder production, the hydriding was carried out at 500 °C, in a high vacuum furnace. After reaching the nominal temperature, the material was hold for 3 hours, under a positive hydrogen pressure. After cooling to room temperature, the friable hydride was milled in a titanium container in vacuum (10^{-2} Torr). Nb, Zr and Ta hydride powders were obtained using the same route; however, hydriding temperatures were significantly higher (800 °C). Table 1 presents the chemical composition of these powders.

The starting powders were weighed (30 grams) and dried for one hour in stove and blended for 30 minutes in a planetary mill with six drips of alcohol. After blending, the powders were cold uniaxially pressed under pressure of 60 MPa, in cylindrical 15 mm dia.-dies. Afterwards, samples were encapsulated under vacuum in flexible rubber molds and cold isostatically pressed (CIP) at 350 MPa during 30 s in an isostatic press.

Sintering was carried out in niobium crucible in high vacuum condition (10^{-7} torr), between 800 and 1600 °C with heating rates of 20 °C/min. After reaching the nominal temperature, samples were hold at the chosen temperature for 2 h and then furnace-cooled to room temperature. Metallographic preparation was carried out using conventional techniques. Specimens were etched with a Kroll solution: 1,5mL HF: 2,5mL HNO₃: 100 mL H₂O to reveal its microstructure. Microhardness measurements were carried out in a Micromet 2004 equipment (Buehler) with a load of 0.2 kgf. The micrographs were obtained using a SEM LEO model 435VPi. The density of the sintered samples was determined by Archimedes method. The micrographs were obtained using a SEM LEO model 435VPi. The specific mass of the sintered samples was determined by Archimedes method, ASTM-C744-74. Particle size distribution was determined by means of laser-scattering equipment (Cilas model 1064). The four points bending tests are performed on an Instron 4301 servo-hydraulic universal testing machine, with a crosshead speed of 0.5 mm/min and load–displacement data were acquired electronically during the test. Samples have a 44 mm length and a 4, 6 mm×4, 1 mm cross-section. The bending strength (σ_B) and the modulus of elasticity, E are calculated using the equations (1) and (2),

where P is the applied load; b and h are, respectively the width and the thickness of the specimen; L and l are the distances between the lower (40 mm) and the upper (20 mm) loading rollers and f is the sample deflection. The expansion/contraction behavior of a Ti-35Nb-7Zr-5Ta during sintering was examined by a dilatometer Netzsch-Dil 402C.s (DEMA-UFSCar).

$$\sigma_B = 3P(L - l) / 2wt^2 \quad (1)$$

$$E = Pa(3L^2 - 4a^2) / f4bh^3 \quad (2)$$

Table 1. Chemical composition of the elemental powders used in this investigation.

Elemental powder	Impurity content (%)				
	N	O	C	Si	Fe
Ti	0,872	0,349	0,073	0,025	0,040
Nb	0,038	0,620	0,020	-	0,040
Zr	0,080	0,450	0,028	-	0,030
Ta	0,150	0,550	0,033	0,030	0,030

3. Results

Table 2 shows the particle size distribution of the elemental powders obtained after hydriding. A great variation of the mean particle sizes between zirconium powders (3 μ m) and niobium and titanium powders (2,5-100 μ m) is observed. This fact has influence on the sintering mechanisms involving the dissolution of the particles, phases stabilization and it is responsible for the final porosity in the samples.

The values of hardness varied in function of the sintering temperature, staying in the range from 100 to 345 HV, while the hardness commonly reported for hot wrought alloys is about 350 HV (Allvac). The samples presented high densification, varying between 69 and 71 % of the theoretical specific mass, after cold isostatic pressing and, among 91 and 93 %, after sintering, with homogeneous microstructure. The theoretical density of Ti-35Nb-7Zr-5Ta alloy is 5,72 g/cm³ [10]. The results of microhardness and specific mass of Ti-35Nb-7Zr-5Ta in function of the sintering temperature were showed in Table 3. In general, the relative specific mass and consequently the microhardness of sintered materials increase when the sintering temperature is raised, because sintering at higher temperatures promotes additional particle-to-particle bonding and more complete alloying because of the higher diffusion rates.

Table 2. Values of particle size distribution of the elemental powders

Elemental Powders	Ti	Nb	Zr	Ta
Particles size (μ m)	31,33	13,80	2,57	25,0

Table 3. Values of microhardness and specific mass in function of the sintering temperature of Ti-35Nb-7Zr-5Ta.

Temperature ($^{\circ}$ C)	Microhardness (HV)	Specific mass
800	100	4,65
900	145	5,02
1000	205	5,11
1100	206	5,33
1200	338	5,40
1300	342	5,47
1400	344	5,58
1500	345	5,68

The microstructural evolution indicates that the homogenization of the alloy is diffusion-controlled (Figure 1). At 800 °C, begins the formation of the β phase regions, starting, in this temperature, mainly from the niobium particles, that act as β -phase nucleator agent. It can be observed that the β structure grows from the niobium diffusion in the neighboring areas consisted of α -titanium particles. The beginning of the stabilization of homogeneous β -areas can be observed at 1100 °C. The microstructure shows that the β -phase formation (plates) has an important role on the samples densification, promoting the bond among the particles and consequently, shrinkage.

The specimen sintered at 1500°C presented the best results when compared to the microstructure found in commercial samples, with a β -homogeneous microstructure and with low porosity. Due the complete dissolution of the alloys elements in the titanium matrix, a good combination of microstructure, mechanical properties and densification could be reached.

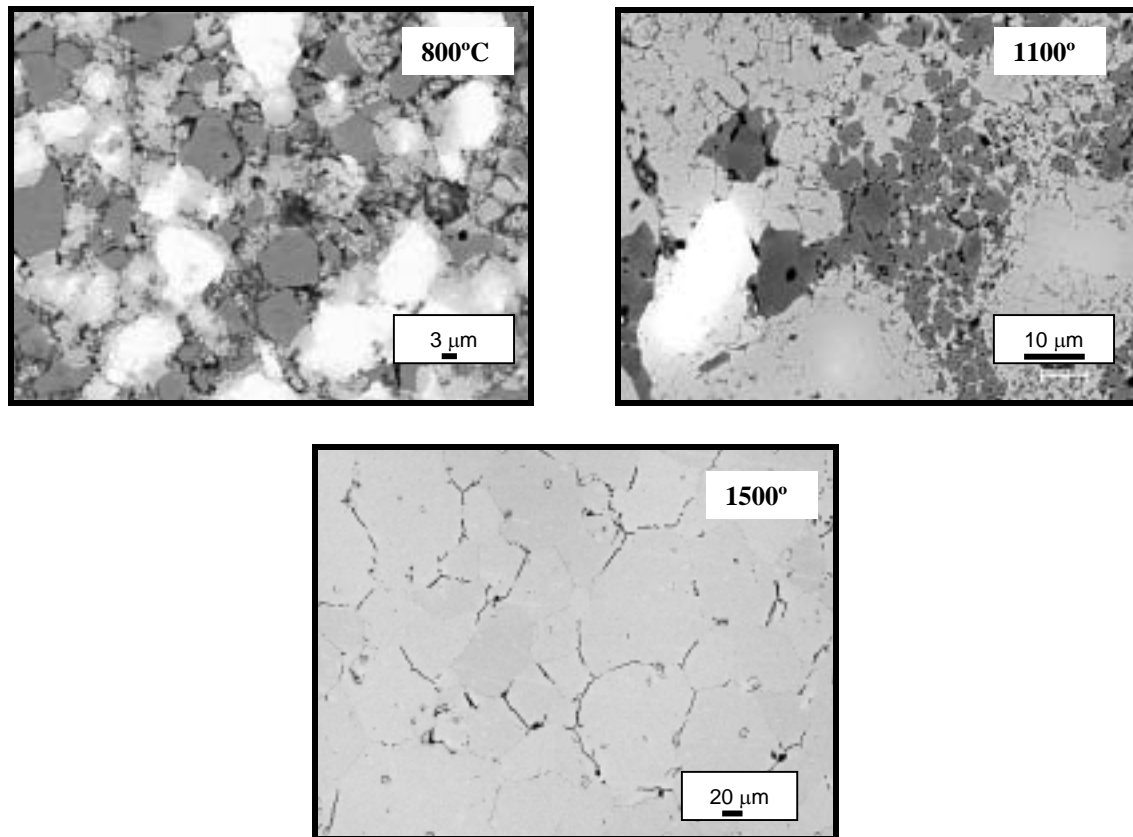


Figure 1. Microstructural evolution of Ti-35Nb-7Zr-5Ta alloy during sintering (for 2 hours and heating rate equal 20 °C·min⁻¹ for all temperatures).

Representative stress–displacement curves obtained from the full-scale four point bending test specimen is represented in Figure 2. The alloy Ti-35Nb-7Zr-5Ta exhibited bending strength around 471, 87 MPa and the modulus of elasticity around 72 GPa, which can be compared to the literature (tensile properties) of 596, 7 MPa and 55 GPa, respectively (Niinomi, 1998).

Figure 3 shows the expansion/contraction behavior of Ti-35Nb-7Zr-5Ta from 200 to 1500 °C. The curve is smooth up to 440 °C. The contraction begins from 440 °C. Densification continued up to 1200°C and overall contraction exceeding 11% was achieved. The contraction starts in a low temperature when compared with

others titanium alloys sintered from dehydrided powders [6]. This fact indicates the influence of hydrogen atoms in the sintering mechanisms providing a contraction even in low temperatures

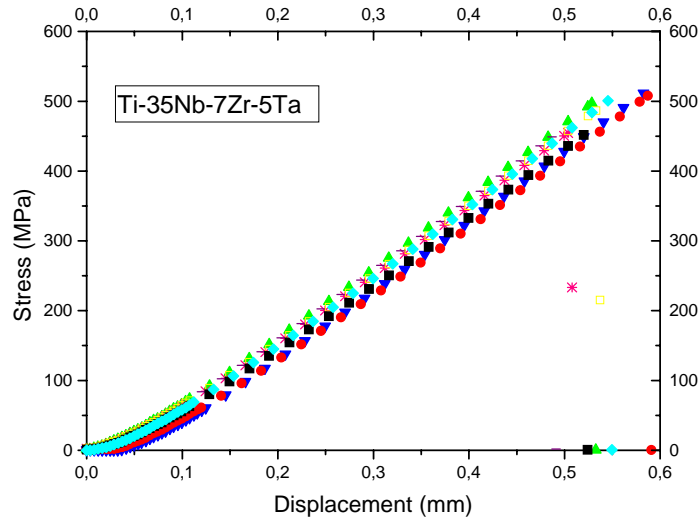


Figure 2. Stress-displacement curves from the four-point bending tests of Ti-35Nb-7Zr-5Ta sintered at 1500 °C.

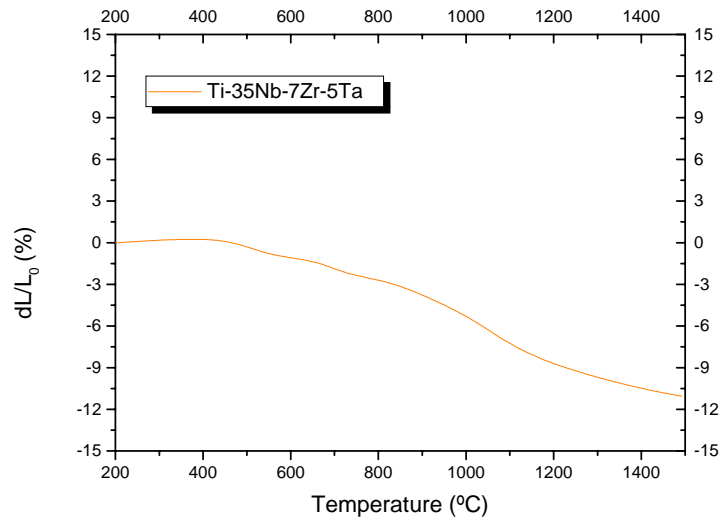


Figure 3. Expansion/contraction behaviour of Ti-35Nb-7Zr-5Ta sintered until 1500 °C.

4. Conclusions

The blended elemental P/M process demonstrated to be efficient for the alloy production. The hydrided powders provided activation in the sintering mechanism promoting contraction in low temperature (400 °C). The samples had presented a good densification and adequate microstructure. The results show that a β -homogeneous microstructure is obtained in the whole sample extension with the increase of the sintering temperature. The hardness values observed in the samples are within the range used in parts produced by

conventional techniques (350 HV). The bend strength and elastic modulus of the alloy provide good conditions for surgical implants utilization.

5. Acknowledgments

The authors wish to thank FAPESP for the scholarship of Taddei, E. B. and DEMAR-FAENQUIL for the Nb and Ta supplying.

6. References

- Allvac, An Allegheny Technologies Company, Catalogue.
- Bora, A., Singha, P.P., Robi, P.S., Srinivasan, A., 2004, "Powder metallurgy processing of ruthenium aluminum alloys", *Journal of Materials Processing Technology* 153–154, pp. 952–957.
- Cahn R. W., Haasen, P., Kramer, E. J, 1991, "Materials Science and Technology-A Comprehensive Treatment", v 15.
- Eisenbarth, E., Velten, D., Muller, M., Thull, R., Breme, J, 2004, "Biocompatibility of β -stabilizing elements of titanium alloys", *Biomaterials* 25, pp. 705–713.
- Fujita, T., Ogawa, A., Ouchi, C., Tajima, H, 1996 " Microstructure and properties of titanium alloy produced in the newly developed blended elemental powder metallurgy". *Materials Science and Engineering A* 213, pp. 148-153.
- Hurless, B.E, Froes, F.H, 2002 "Lowering the cost of Titanium", *The AMPTIAC Quarterly*, V6, number 2.
- Katti, K. S., 2004, "Biomaterials in total joint replacement", *Colloids and Surfaces B: Biointerfaces*, Volume 39, Issue 3, 10 December , pp. 133-142.
- Long, M.; Rack, H.J, 1998 "Review Titanium Alloys in Total Joint Replacement-A Materials Science Perspective". *Biomaterials*, 19, pp. 1621-1639.
- Niinomi, M, 1998 "Mechanical properties of biomedical titanium alloys", *Materials Science and Engineering: A*, Volume: 243, n. 1-2, pp. 231-236.
- Popa, M. V., Demetrescu, I., et al, 2004, "Corrosion susceptibility of implant materials Ti–5Al–4V and Ti–6Al–4Fe in artificial extra-cellular fluids". *Electrochimica Acta* 49, pp. 2113–2121.
- Watarai, F., Yokoyama, A., Omori, M., Hirai, T., Kondoa, H., Motohiro Uo, Kawasaki, T, 2004, "Biocompatibility of materials and development to functionally graded implant for bio-medical application". *Composites Science and Technology* 64, pp. 893–908.